6. Kon, S., J.R. Wagner, D.G. Guadagni and R.J. Horvat, J. Food Sci. 35:343 (1970).
7. Smith, A.K., and S.J. Circle, Soybeans: Chemistry and Technology, Volume 1, Proteins, AVI Publishing Co., Westport, CT, 1972.
8. Aguilera, J.M., E.W. Lusas, M.A. Uebersax and M.E. Zabik, J. Food Sci. 47:996 (1982).
9. Aguilera, J.M., E.W. Lusas, M.A. Uebersax and M.E. Zabik, Ibid. 47:1151 (1982).
10. AACC, Approved Methods, 7th ed., American Association of Cereal Chemists, St. Paul, MN, 1962.
11. Robertson, J.B., and P.J. Van Soest, J. Anim. Sci. 45 (Suppl. 1): 254 (1977).
12. Patel, K.M., C.L. Bedford and C.W. Youngs, Cereal Chem. 57: 123 (1980).
13. Sahasrabudhe, M.R., J.R. Quinn, D. Paton, C.G. Youngs and B.J. Skura, J. Food Sci. 46:1079 (1981).
14. Fogg, N.E. and G.L. Tinklin, Cereal Sci. Today 17:70 (1972).
15. Rooney, L.W., C.B. Gustafson, S.P. Clark and C.M. Calth, J. Food Sci. 37:14 (1972).
16. Khan, M.N., and J.T. Lawhom, Cereal Chem. 57:433 (1980).
17. Volpe, T.A., and M.E. Zabik, Ibid. 58:441 (1981).
18. D'Appolonia, B.L., Bidi. 55:898 (1978).

[Received October 19, 1982]

⁂Computer Modeling of Theoretical Structures of Monoacid Triglyceride α-Forms in Various Subcell Arrangements

J.W. HAGEMANN and **J.A. ROTHFUS**, Northern Regional Research Center, Agricultural Research Service, US Department of Agriculture, Peoria, IL 61604

ABSTRACT

Six theoretical triarachidin space-filling α-form structures were examined using a computer modeling technique that simulated restricted oscillations of carbon zigzag planes in synchronous and nonsynchronous modes. Intermolecular minimization procedures determined best-fit positions around a centralized molecule, which enabled calculation of total lattice energy values for nine different hexagonal subcell arrangements. Subcell arrangement had a greater effect on the energy of the system than did the configuration of the triglyceride. The analysis thus far indicates several equally preferred structure-subcell arrangement combinations for triglyceride α-forms rather than a single crystalline entity.

INTRODUCTION

Knowledge of the molecular conformation and three-dimensional packing of triglycerides in different crystal forms is fundamental to understanding lipid phase behavior. It is obvious that these solid-state structures play a vital role not only in fat processing but also in organized structures of biological systems. Yet after years of research, the molecular conformation is known for only the β-form (highest melting) (1), which represents essentially one-third of the overall picture also involving the α-form (lowest melting) and β′-form (intermediate melting) (2). Although X-ray diffraction (3–5), infrared spectroscopy (6), nuclear magnetic resonance (7) and thermal analysis (4, 8, 9) have contributed substantially to the knowledge of α- and β′-forms, their elusive crystal structures and molecular packing characteristics have escaped these investigations. Computer modeling, an alternative procedure that can provide insight into molecular arrangements, has been applied to lipids primarily for intramolecular conformational analysis of phospholipids (10) and short-chain triglycerides (11, 12). The current study emphasizes intermolecular interactions because they were previously successful in accounting for structural relationships and stabilities among *n*-hydrocarbons (13). Like hexagonal hydrocarbons, α-form triglycerides can be considered the first of several forms in a chain of events leading eventually to stable β-forms. Because of its orthogonal structure and similarity to the triglyceride liquid state (5), the α-form represents a convenient starting point. We thus modeled various theoretical conformers of α-triarachidin for comparative lattice energy information on both the structure and packing arrangements.

On cooling from the melt, most long-chain compounds transform into a hexagonal crystal structure with the chains possessing rotational freedom about longitudinal axes. In triglycerides, the acyl methylene chains are considered to perform restricted rotation or oscillatory motion because of their attachment to the polar glycerol region, but small oscillations take up the same amount of space as complete rotation (7). The α-form melting points (4, 9) and X-ray long spacings (4) of triglycerides do not alternate between even and odd chainlengths, thereby suggesting vertical acyl methylene chains with respect to the end group planes, in contrast to β′- and β-forms with tilted chains. Since β- and/or β′-forms are rapidly made from the α-form, any theoretical α-form structures are likely to be in the tuning-fork type configuration of the β-form and alternate between upright and inverted positions of adjacent molecules (1). An understanding of the configurational and position arrangement possibilities for the α-form and the techniques to obtain them will allow for prediction and validation of structures and pathways to β′- and β-forms and other new forms recently discovered (9).

EXPERIMENTAL

α-Form Structures

A triglyceride model was constructed of trioctanoin using the Minit Model System (Science Related Materials, Inc., Janesville, WI) having a scale of 1.25 cm/Å. By manipulation of the bonds around the glycerol region and, at the same time, maintaining an all *trans* configuration of the acyl chains, a symmetrical tuning-fork conformation was found (Fig. 1A) that allowed the length of the molecule to approximate closely the recorded long spacing for the α-form (4). The atomic coordinates of atoms were determined using bond lengths and angles reported for the single crystal of the trilaurin β-form (1). A distinguishing feature of the molecule is that the carbon zigzag plane of chain 2 is approximately perpendicular, or nonparallel, to the carbon zigzag planes of chains 1 and 3. Also, a plane bisecting the

center of chain 2 is close to the mid-chain distance between chains 1 and 3.

Some hindrance to rotation occurs about the carbonyl carbon and the ester oxygen bond of chain 2, not only because of resonance structures (15) but also because of van der Waals radii overlap between the glycerol β-hydrogen atom and the carbonyl oxygen. This steric hindrance is easily observed with space-filling models such as the precision CPK molecular models (The Ealing Corp., Cambridge, MA). As a result, the carbonyl oxygen is likely to be located on one side or the other of the β-hydrogen rather than in opposition to it. Several other orientations of chain 2 are, therefore, possible without changing the positions of chains 1 and 3. The carbon zigzag plane of chain 2 can be approximately perpendicular (Fig. 1A and D) or parallel (Fig. 1B and E) to the other two carbon zigzag planes, whereas at the same time, the carbonyl oxygen can be to the right or left (as shown in Fig. 1) of the β-hydrogen on glycerol. Another variation is that chains 1 and 3 can exhibit an opposite carbon zigzag pattern as shown in Figure 1C and F. These structures differ from the unsymmetrical tuning-fork model proposed recently (16) for α-forms.

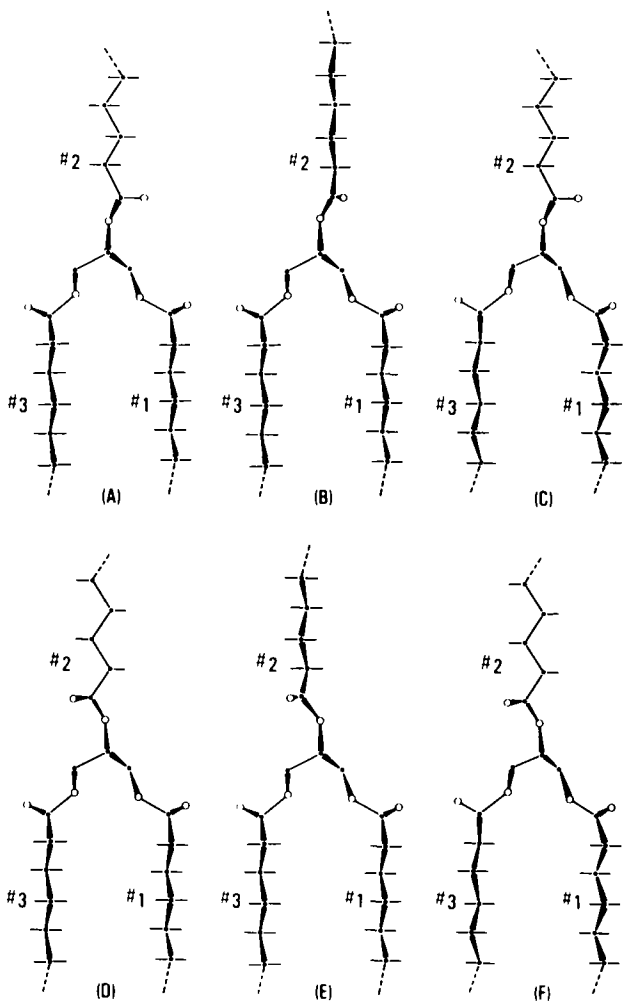

FIG. 1. Triglyceride α-form structures used in the computer modeling studies. Carbon atoms are indicated as solid circles, oxygen atoms as open circles. Some hydrogen atoms are indicated as lines from carbon atoms. Chains are numbered according to the convention of Lutton (14).

The six α-form structures shown in Figure 1 were used as the starting molecules of triarachidin for computer modeling studies. Structures in this report will be referred to as having parallel or nonparallel chains, carbonyl right or left and the same or opposite zigzag.

Calculation of Interaction Energies

A rotational movement in the hydrocarbon chains was incorporated into the model to simulate the oscillatory motion about the long axis in α-forms. The methyl and methylene groups were rotated out of the zigzag plane as shown in Figure 2. Rotation out of the zigzag plane was greatest at the ends of the chains and least nearest the glycerol moiety producing a cone-shaped surface (Fig. 2A). The maximum displacement from the original zigzag plane starting position for the methyl carbons was 60° (Fig. 2B). After reaching this maximum, the zigzag plane rotated back to the starting position and proceeded to the −60° position. In this manner an oscillatory motion was produced where the individual chains could be rotated in or out of synchrony. For synchronous oscillation, rotation of each chain was in 2° increments; for nonsynchronous oscillation, rotation increments for chains 1, 2 and 3 were 2°, 4° and 6°, respectively. The maximum difference between adjacent carbon atoms when at the ±60° positions was slightly over 3°.

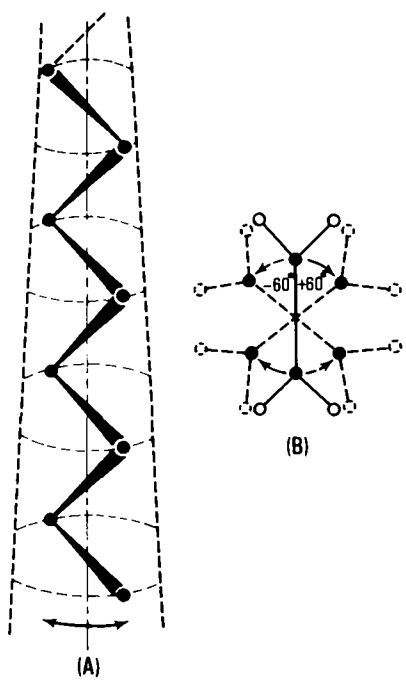

FIG. 2. Diagrams of restricted oscillations employed in hydrocarbon chain segments of triarachidin. Carbon atoms are indicated as solid circles, hydrogen atoms as open circles. (A) Side view of chain oscillation about long axis of carbon zigzag plane. (B) End view of chain oscillation. Maximum displacement of ±60° occurs only with methyl groups. See text for details.

A flow diagram of the Fortran IV computer program used to determine the position and lattice energy between pairs of triglyceride molecules in hexagonal arrangements is shown in Figure 3. After the degrees of rotation were determined for each chain, the appropriate carbon atoms and their attached hydrogens were rotated and their new

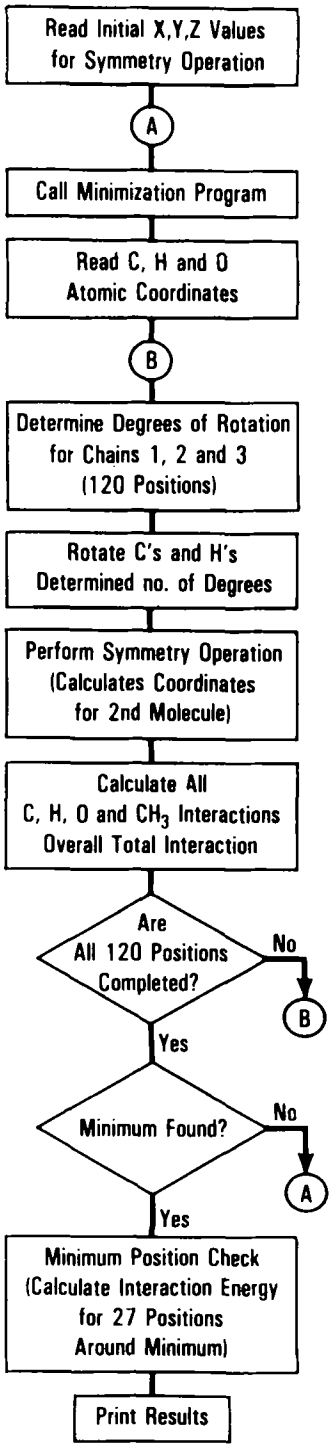

FIG. 3. Flow diagram of computer program for calculation of interaction energies between pairs of oscillating triglyceride molecules.

atomic coordinates were calculated. A predetermined symmetry operation was performed whereby atomic coordinates were calculated for all atoms of a second molecule. All atom-atom interaction potentials were calculated according to the procedure of Coiro et al. (17) except for CH_3-O interactions which, for triarachidin, would all lie beyond the 6 Å cut-off distance. The total of all interaction potentials was summed for a final value. This procedure was repeated for 120 positions of the methylene chains (chain 1 methyl group, for 2° increments, would rotate from the starting position to +60° to −60° and back to starting position). After all 120 positions were completed, a final average of all 120 values was given for all interactions between the two triarachidin molecules.

A minimization program (18) was utilized whereby the starting x, y and z axis coordinates, representing a symmetry operation for the second molecule, were varied depending on total interaction values obtained from previous runs of the 120 positions. The minimization subroutine was in effect until a minimum energy position of the second molecule with respect to the first was located. The position of the minimum was checked by incrementing the final x, y and z values by 0.1 Å. If this increment produced no greater minimum, the position and value were recorded. If a greater minimum were found, those new coordinates were inserted as starting points and the entire process was repeated.

RESULTS

Hexagonal Subcell Arrangements

Most pictorial descriptions of the hydrocarbon chain subcell packing in triglycerides (5) depict the general arrangement of individual zigzag chain planes with respect to neighboring ones. However, since triglycerides occur in a tunning-fork type configuration where two of the chains are on the same side of the molecule (chains 1 and 3 in Figure 1), some symbol is needed in subcell drawings to indicate whether chains belong to the same or different molecules. Because the tuning-fork structure alternates between adjacent molecules with chain 2 pointing upright or inverted downward (1), it is necessary to indicate only one-half of the triglyceride molecule to show the position of the entire molecule. Therefore, the carbon zigzag planes of chains 1 and 3 have been represented as two connected zigzag carbon planes and the plane of chain 2 as an individual zigzag plane. The arrangements in Figure 4 are not intended to show actual subcell packing of the acyl methylene chains but to indicate relative positions of entire molecules.

In the hexagonal subcell packing, chains are oriented to form a six-sided figure producing angles of ca. 120°. Assuming the alternating structures previously mentioned and parallel rows of molecules, it is possible to describe nine different arrangements of molecules in hexagonal packing (Fig. 4). A principal or central molecule used as a starting point, from which all intermolecular calculations were performed, is labeled P in row 2 of each arrangement. A typical hexagonal orientation involving seven zigzag planes (the seventh being in the center) is enclosed with dotted lines in each arrangement. The center of each zigzag chain is ca. 5 Å from adjacent chains in all directions (18).

The P molecule in the middle row, therefore, is an upright tuning-fork molecule between two inverted molecules and is the same for all arrangements. By keeping row 3 constant relative to row 2, three different arrangements are possible (Fig. 4; 1, 2 and 3), by moving the molecules in row 1. Likewise, by moving row 1 relative to row 2 following a shift of row 3 relative to row 1, three additional arrangements are produced: 4, 5 and 6. Repetition again gives arrangements 7, 8 and 9. Although at first glance some of the arrangements appear to be the same, i.e., 2 and 4, 3 and 7, they are neither minor images nor superimposable because the triglyceride molecule is not symmetrical. Although row 1 of 2 and row 3 of 4 appear identical, they each present different sides of the molecules to row 2, assuming no complete revolution of entire molecules, and face a different side of row 2.

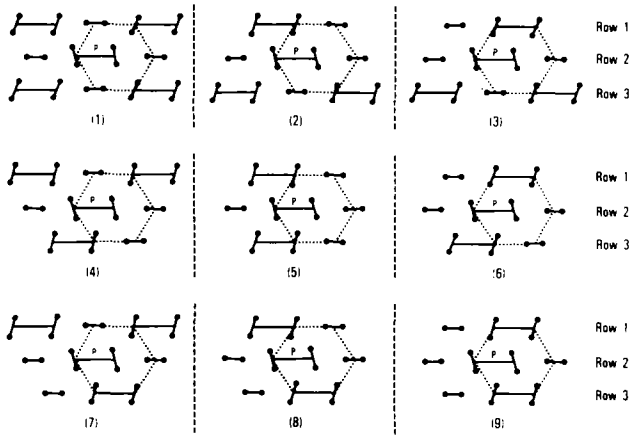

FIG. 4. Possible arrangements of triglyceride molecules in hexagonal subcell packing. One zigzag period is shown in the direction of the hydrocarbon chains. Connected zigzag periods represent chains 1 and 3 from the same molecule, individual zigzag periods represent chain 2 from a separate molecule. Carbon atoms are shown as closed circles, hydrogen atoms are not indicated.

The coordinate system for the arrangements in Figure 4 are x-axis, horizontal, y-axis, vertical and z-axis, perpendicular to the paper. Chains 1 and 3 in rows 1 and 3 represent a reflection of the central molecule (P) in the x-direction ($\bar{x}$), and four different positions with respect to molecule P are possible. The inverted molecule or chain 2 is meant to represent either parallel or nonparallel chain structures, the nonparallel type being depicted in Figure 4. In rows 1 and 3, three positions of chain 2 are possible. Molecules represented by chain 2 were obtained by reflection of molecule P in the z-axis direction ($\bar{z}$). Inverted molecule positions were determined for both x, a translation of the entire molecule, and $\bar{x}$ symmetry operations. All molecules in the nine arrangements have all or part of their structures within 6 Å of all or part of molecule P.

Preferred Energy Positions

Although three positions are shown for chain 2 in rows 1 and 3, only one position has maximum interaction with molecule P in each row. This position is located approximately midway between chains 1 and 3 of molecule P as shown in arrangement 1. Likewise, molecules represented by chains 1 and 3 are shown in four different positions in each of rows 1 and 3. Yet only two positions in each row, represented in arrangements 6 and 8, have maximum interaction with molecule P. When starting positions for the second molecule were somewhat removed from P, the computer minimization program moved the molecule to the above mentioned positions. Positions of molecules shown removed from P in Figure 4 were determined using the four maximum interaction energy positions for the upright and the four positions (two in row 2) for the inverted molecules.

A cutoff distance of 6 Å in the molecular interaction calculations limits the number of molecules having all or part of their atoms within this distance from all or part of the atoms of molecule P. As shown in Figure 4, one arrangement has eight molecules around P, four have seven and four have six. Not shown are molecules above and below molecule P across the methyl gap to which interactions were also calculated.

The above-described maximum interaction energy positions are those located in the x-y plane. The maximum energy positions found for adjacent molecules along the long axis of the molecule, z-axis, are not those expected for nontilting chains. Most of these positions show chains from different molecules to be offset in such a way that methyl groups lie above or below those in molecule P. This allows protons from one chain to fit in between protons from a second chain. However, since triglycerides in the α-form possess no angle of tilt (7), these positions are not real for hexagonal arrangements but may play an important role in tilted chain structures. Positions with methyl groups in the same plane as those on molecule P were found by manual manipulation of the x-y coordinates.

Although the molecules are shown lined up horizontally in Figure 4, the actual minimum energy positions for the inverted molecules in row 2 were often shifted in the ±y-direction from a few tenths of an Å to as much as ±3.7 Å. Since the position of each molecule was determined from interaction with just one other molecule, the position found would not necessarily represent its final position in the overall array due to the influence of surrounding molecules. For the inverted molecules in row 2, the $\bar{x}$ structure was preferred more often than x in both positions for all six structures, whereas x was favored in rows 1 and 3. The z-axis positions favored for the upright molecules were ca. ±2.5 Å for all structures in synchronous and nonsynchronous oscillation. This corresponds closely to the z-axis repeating unit found in crystallographic studies of long-chain hydrocarbon type structures (19).

A typical energy contour map showing the interaction between two molecules relative to position is illustrated in Figure 5. The two minima depicted were those found when an upright molecule in row 1 of Figure 4 was moved across the stationary P molecule in the x-direction at various distances from the P molecule, y-direction. The z-axis coordinate for all data points was 0.0. As shown in Figure 5, the energy profile is quite flat when the two molecules are separated by 5.0 Å. As the intermolecular distance becomes less, a repulsive energy section appears at approximately the center of molecule P producing the two positions of maximum attractive energy. Resolution on the x-axis was 0.1 Å and on the y-axis, 0.05 Å. Higher resolution would show the minor undulations present in the contour lines which necessitated the minimum position check (Fig. 3).

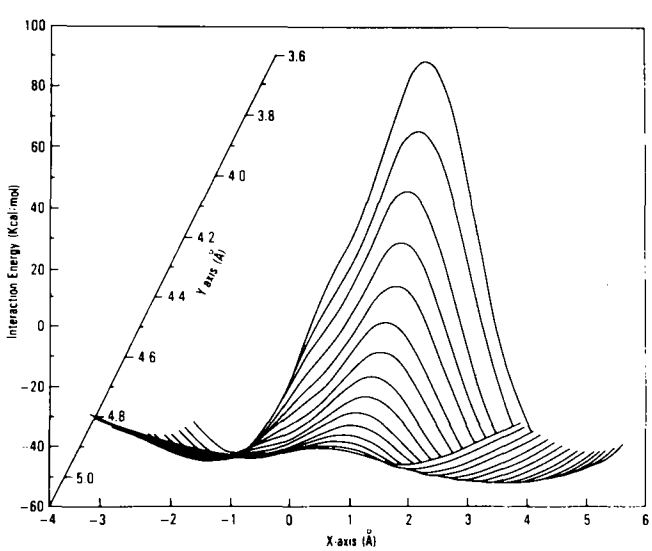

FIG. 5. Molecular interaction energy contour map showing minima as an upright triglyceride molecule is moved across a stationary upright molecule. Data are from a synchronous oscillating model.

Subcell Arrangement Energies

Even though chain oscillations occur in triglyceride α-forms, which would cause subcells not to show parallel zigzag planes as depicted in Figure 4, the higher melting forms, β'- and β, do have parallel chains in alternate rows in β' and in all rows in β. Since infrared studies have suggested similarity between α- (hexagonal) and β'-forms (orthorhombic) (6, 20), it is not unlikely to assume that a stop-action picture of hexagonal packing might also show parallel chains in each row. In order to achieve this, upright triglycerides in rows 1 and 3 of Figure 4 require an $\bar{x}$ symmetry operation; hence, the reason for only x calculations with chains 1 and 3 down. And although structures B and D of Figure 1 are referred to as parallel chain structures, the slight twist of chain 2 with respect to chains 1 and 3 requires $\bar{x}$ operation in row 2 of Figure 4 and x operation in rows 1 and 3 to achieve parallelism with chains 1 and 3. Therefore, the results reported were obtained from alternating x and $\bar{x}$ structures in each row. The symmetry operation would not have a large effect on chain 2 for nonparallel chain structures. For consistency, alternation of x and $\bar{x}$ for inverted molecules of nonparallel chain structures was also performed.

The energies of interaction for each position in Figure 4 were summed to obtain a total value for each subcell arrangement. Results obtained for each structure in Figure 1 are shown in Table I. Included in these totals are 5–6 kcal/mol from interactions to parts of eight methylene chains across the methyl gaps at opposite ends of the molecule. Early results with structures A, B and E revealed that synchronous oscillation generally gave slightly higher interactions (greater negative attractive values) as seen in the average/arrangement values at the bottom of Table I. Therefore, nonsynchronous oscillation values were not obtained for the two opposite zigzag structures, C and F. Structure A had the highest average/arrangement and the least spread in energy values over the nine arrangements. Structure F produced quite different results due to some repulsive 0-0 values in inverted molecules to the upper right and lower left of molecule P (Fig. 4) even though the same basic eight positions were used to calculate those outer positions as with the other structures. Thus, for structure F, arrangement 8 gave a repulsive value producing a range in values of almost 193 kcal/mol. Figure 6 presents graphically the results in Table I for structures A, B, D and E. It is obvious that all of the arrangements of structure A have approximately the same energy content, with arrangements 8 and 9 representing the best fit. Structure E has two arrangements with energy matching that of structure A, but it also has arrangements not far removed from the low energy ones of structure B. Overall, the general patterns for nonsynchronous oscillation were very similar to those for synchronous oscillation.

Once all the best fit positions were found for all structures, additional runs were made at all positions to determine the contribution of each type of interaction for each atom. Having these results, the contribution of individual methylene groups within the chains could be calculated. By adding or removing methylene unit contributions, extrapolation to other chain lengths was possible in addition to calculation of a middle-of-chain contribution for each fatty acid chain. Middle-of-chain is defined as the methylene units in each chain that do not have any interaction to oxygen or methyl groups but only to other methylene units. This contribution for each chain of several structures having arrangements of high interaction energy is shown in Table II. Only arrangement 6 of structure C did not have chain 2 as the greatest contributor to the overall energy. The opposite zigzag on chain 3 of structure C had a greater con-

TABLE I

Total Interaction Energies of Hexagonal Subcell Arrangements[a]

Subcell arrangement from Figure 4	Structure[b] A		Structure B		Structure C	Structure D		Structure E		Structure F
	Nonsyc	Syc	Nonsyc	Syc	Syc	Nonsyc	Syc	Nonsyc	Syc	Syc
1	−194.6	−196.4	−178.4	−179.7	−181.9	−169.8	−168.3	−175.6	−184.4	−163.7
2	−200.4	−202.2	−178.6	−179.6	−184.3	−168.1	−166.9	−162.5	−169.7	−90.2
3	−201.3	−202.9	−185.9	−187.5	−187.2	−176.3	−175.1	−174.5	−184.0	−146.0
4	−197.6	−197.2	−160.5	−160.9	−185.2	−184.7	−182.1	−198.1	−204.8	−158.7
5	−203.4	−203.0	−160.8	−160.8	−187.6	−183.0	−180.6	−185.0	−190.1	−85.2
6	−204.3	−203.7	−168.0	−168.7	−190.5	−191.2	−188.9	−197.0	−204.4	−141.0
7	−199.6	−202.3	−190.1	−191.3	−189.2	−169.1	−170.3	−175.5	−181.8	−44.4
8	−205.4	−208.1	−190.4	−191.2	−191.6	−167.4	−168.9	−162.4	−167.1	+29.2
9	−206.3	−208.8	−197.6	−199.1	−194.5	−175.6	−177.2	−174.4	−181.4	−26.7
Average	−201.4	−202.7	−178.9	−179.8	−188.0	−176.1	−175.4	−178.4	−185.3	−91.9
Δ Energy[c]	11.7	12.4	37.1	38.3	12.6	23.8	22.0	35.7	37.7	192.9

[a]Energy results (17) are expressed in kcal/mol. Values include calculations across methyl gaps. The more negative attractive values represent more stable or preferred arrangements.
[b]Structure identifications are from Figure 1.
[c]Range in total energy values of the nine arrangements.

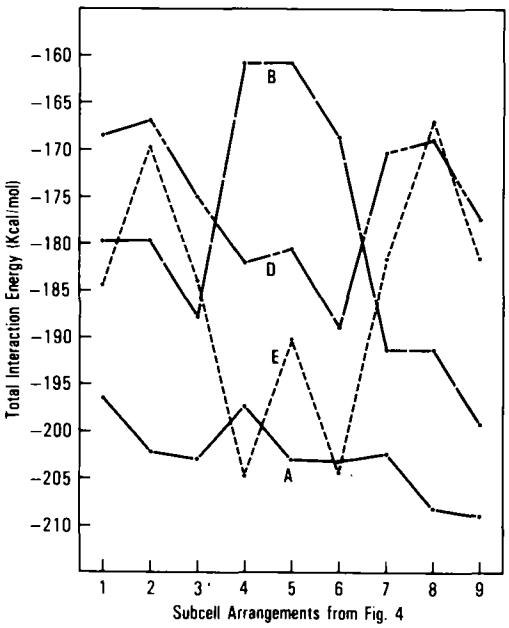

FIG. 6. Subcell arrangement vs total interaction energy for synchronous oscillation. Structure identification on the lines are from Fig. 1.

tribution than chain 3 of structure A, and the total contribution was also higher. Even though arrangement 9 of structure A had the greatest total interaction energy, arrangement 8 had a greater middle-of-chain contribution. It is, therefore, obvious that some arrangements contribute more at the polar region, because the methyl gap contribution was relatively constant for all structures and arrangements. For *n*-alkanes (13), solid phase changes from triclinic to monoclinic occurred, and stability of α-forms increased when the middle-of-chain contribution was near or exceeded 60%. With triglyceride α-forms, extrapolation to longer chains revealed that the middle-of-chain contribution of 60% occurs at C_{24}.

DISCUSSION

The search for configurational answers to the α-form structure of triglycerides must be based on projections of knowledge gained previously not only from the triglyceride β-form but from other long-chain molecules. Assumptions mentioned earlier were rows of parallel zigzag planes, alternating zigzag planes in successive rows, alternating upright and inverted molecules and symmetrical tuning-fork molecules. An even more significant constraint, perhaps, is that chains 1 and 3 were both placed in the same row (Fig. 4) and not in different rows. Although out-of-plane configurations like those seen occasionally with hydrocarbons (21) are possible (since all chain centers are approximately the same distance apart), their inclusion here would have made the number of possibilities exorbitant. Even with the above limitations, the six structures in this study with the nine subcell arrangements and synchronous and nonsynchronous oscillations result in a sizable number of combinations. Reality may be a much simpler picture, because order in the near-crystalline liquid state prior to solidification may be an important determinant of subsequent polymorphic behavior.

The β-form, which has parallel chain planes tilted with respect to the methyl plane, is known to be the most stable structure of saturated monoacid triglycerides. Some of the data obtained for the α-form structures support the fact that the β-form is a more preferred structure. Structures B and E (Fig. 1) are unsymmetrical, with chain 2 not bisecting the space between chains 1 and 3. They resemble the β-form somewhat. Structure E showed preference for parallel chains; i.e., two subcell arrangements, 4 and 6 (Fig. 6) were among the highest subcell energies found. The orientation of chain 2, whether parallel or nonparallel with chains 1 and 3, did not have a significant effect on the total subcell energies. Chain orientations do, however, affect the contribution that individual chains produce by interaction with adjacent molecules. Comparisons of structures A and C (Table II) reveal that the middle-of-chain contribution for chains 1 and 3 increase for structure C over those of structure A when the carbon-carbon zigzag pattern for chain 3 is reversed (Fig. 1). This allows for a better fit of protons on adjacent chains that do not as readily come in close contact for repulsive interaction. Thus, the overall positioning of the molecules in the subcell has a far greater effect on the total energy (Table I) than the orientation of individual chains. Additional preference toward β-form types was evidenced by the fact that preferred z-direction positions favored arrangements that would produce angles of tilt across end group planes. Although these positions were not used for this report, they may be indicative of possible routes toward formation of β′- and/or β-forms.

TABLE II

Contribution (%) of Middle-of-Chain Energy to Total Subcell Energy

Triglyceride structure from Figure 1	Chain no. 1	2	3	Total	Extrapolate[a] C_{16}	C_{24}	Chain no. 1	2	3	Total	Extrapolate[a] C_{16}	C_{24}
	Subcell 4[b]						Subcell 6					
A							15.0	19.1	15.4	49.5	38.8	57.2
C							17.1	15.6	18.3	51.0	40.3	58.4
E	16.7	17.6	15.3	49.6	39.1	57.1	16.6	18.1	16.4	51.1	40.8	58.3
	Subcell 8						Subcell 9					
A	16.9	20.9	14.7	52.5	42.2	59.6	16.6	19.6	14.7	50.9	40.2	58.4
C	17.3	19.7	16.1	53.1	42.8	60.4	18.2	18.5	16.1	52.8	42.4	60.2

[a]Energy calculations for chainlengths other than C_{20} by addition or subtraction of methylene units. See text.
[b]Subcell numbers are from Figure 4.

The similarity observed for total subcell energies between synchronous and nonsynchronous oscillation was an unexpected result. Certainly, small oscillations must occur in orthorhombic and triclinic structures, but the close proximity of chains would require that efficient interspacing be a necessity. It is obvious that a meshed-gear type motion would be more important with closely packed chains than in a more loosely packed array. Presumably the interchain spacing in hexagonal subcells minimizes van der Waals overlap and allows nonsynchronous oscillation.

Recent results from differential scanning calorimetry of single acid triglycerides (9) showed multiple α-forms for fatty acid chainlengths of C_{20} and greater. The diversity of preferred structures and subcell arrangements found in the current work would allow for many forms at all chainlengths. Due to greater methylene interaction at longer chainlengths (Table II), many arrangements that are not stable for shorter chainlengths could be stable for larger molecules, thus accounting for multiple forms observed.

Having results for some 90 combinations of structures and subcell arrangements, it is tempting to speculate as to the preferred combination for triglyceride α-forms. However, there is no single combination that stands out among the rest. Certainly, all arrangements for structure A are preferred (Fig. 6), along with arrangements 4 and 6 of structure E and arrangement 9 of structure B. A more likely conclusion is that there is no single structure and/or subcell arrangement for α-forms but a mixture of many arrangements, perhaps enriched by several more preferred structures. Interaction in the near-crystal may help direct the population into one or more of these preferred structures. A mixture would account for their instability, low heats of fusion, broad melting characteristics (8, 9) and their inability to form single crystals. The levels and ranges of interaction energy for the structure and arrangement combinations provide many pathways for solid transitions to occur from more stable to less stable forms during α-form activation and transformation to higher melting polymorphs. Unknown yet is what role these combinations might play in determining the paths taken, respectively, by odd or even chain length triglycerides to either β′- or β-forms, which exhibit substantially different X-ray characteristics (4) and thermal behavior (9).

ACKNOWLEDGMENT

The authors thank the NRRC computer staff, R.O. Butterfield and D.J. Wolf, for their valuable assistance and advice during the course of this work.

REFERENCES

1. Larsson, K., Ark. Kemi. 23:1 (1965).
2. Chapman, D., Chem. Rev. 62:433 (1962).
3. Hoerr, C.W., JAOCS 41:4, 22, 32, 34 (1964).
4. Lutton, E.S., and A.J. Fehl, Lipids 5:90 (1970).
5. Larsson, K., Fette, Seifen, Anstrichm. 74:136 (1972).
6. Chapman, D., JAOCS 37:73 (1960).
7. Larsson, K., Ark. Kemi. 23:35 (1965).
8. Hagemann, J.W., W.H. Tallent and K.E. Kolb, JAOCS 49:118 (1972).
9. Hagemann, J.W., and J.A. Rothfus, JAOCS 60:1123 (1983).
10. McAllister, J., N. Yathindra and M. Sundaralingam, Biochemistry 12:1189 (1973).
11. Govil, G., R.V. Hosur and A. Saran, Chem. Phys. Lipids 21: 77 (1978).
12. Hosur, R.V., A. Saran and G. Govil, Indian J. Biochem. Biophys. 16:165 (1979).
13. Hagemann, J.W., and J.A. Rothfus, JAOCS 56:1008 (1979).
14. Lutton, E.S., JAOCS 48:245 (1971).
15. Piercy, J.E., and S.V. Subrahmanyam, J. Chem. Phys. 42:1475 (1965).
16. Hernqvist, L., and K. Larsson, Fette, Seifen, Anstrichm. 84: 349 (1982).
17. Coiro, V.M., E. Giglio, A. Lucano and R. Puliti, Acta Crystallogr. B29:1404 (1973).
18. Rosenbrock, H.H., and C. Storey, Computational Techniques for Chemical Engineers, Pergamon Press, 1966, pp. 64–68.
19. Larsson, K., JAOCS 43:559 (1966).
20. Chapman, D., J. Chem. Soc. 4489 (1957).
21. Scherer, J.R., and R.G. Snyder, J. Chem. Phys. 72:5798 (1980).

[Received November 9, 1982]